Carbohydrate Polymers 115 (2015) 93–103

Contents lists available at ScienceDirect

Carbohydrate Polymers

journal homepage: www.elsevier.com/locate/carbpol

Combining FT-IR spectroscopy and multivariate analysis for qualitative and quantitative analysis of the cell wall composition changes during apples development

M. Szymanska-Chargot*, M. Chylinska, B. Kruk, A. Zdunek

Institute of Agrophysics, Polish Academy of Sciences, Doswiadczalna 4, 20-290 Lublin 27, Poland

ARTICLE INFO

Article history:
Received 27 June 2014
Received in revised form 7 August 2014
Accepted 8 August 2014
Available online 27 August 2014

Keywords:
Plant cell wall
Polysaccharides
FT-IR
Spectroscopic analysis
Chemometry

ABSTRACT

The aim of this work was to quantitatively and qualitatively determine the composition of the cell wall material from apples during development by means of Fourier transform infrared (FT-IR) spectroscopy. The FT-IR region of 1500–800 cm^{-1}, containing characteristic bands for galacturonic acid, hemicellulose and cellulose, was examined using principal component analysis (PCA), *k*-means clustering and partial least squares (PLS). The samples were differentiated by development stage and cultivar using PCA and *k*-means clustering. PLS calibration models for galacturonic acid, hemicellulose and cellulose content from FT-IR spectra were developed and validated with the reference data. PLS models were tested using the root-mean-square errors of cross-validation for contents of galacturonic acid, hemicellulose and cellulose which was 8.30 mg/g, 4.08% and 1.74%, respectively. It was proven that FT-IR spectroscopy combined with chemometric methods has potential for fast and reliable determination of the main constituents of fruit cell walls.

1. Introduction

The composition of cell walls in fruits is important for both consumers and industry (Billy et al., 2008; Cybulska, Zdunek, Psonka-Antonczyk, & Stokke, 2013). From the consumer perspective, cell walls in fruits are a valuable source of dietary fibres (Phillips & Cui, 2011; Brownlee, 2011) and they determine the texture of fruits thereby largely influencing their sensory acceptability (Cybulska et al., 2013; Li et al., 2013). For industry, cell walls from fruits are a valuable source of pectins and are responsible for the effectiveness of many technological processes (Willats, Knox, & Mikkelsen, 2006). Therefore, knowledge about cell wall composition, that is, understanding the actual fruit texture properties and very pronounced changes that take place during fruit development and maturation, is critical.

In the primary plant cell walls, cellulose microfibrils are embedded in a highly hydrated matrix composed of hemicelluloses and pectins with the addition of structural proteins. Generally, it is believed that the primary cell wall is composed of approximately 25% cellulose, 25% hemicellulose and 35% pectins, with up to 8% structural proteins (on a dry weight basis). However, large deviations from these values may be found (Taiz & Zeiger, 2002).

Cellulose microfibrils are relatively stiff structures that contribute to the strength and structural bias of the cell wall. A single cellulose chain is composed of β(1,4)-linked glucan chains which are tightly aligned and bonded to each other so as to create a highly ordered, crystalline fibril. That structure excludes water and is relatively inaccessible to enzymatic attack, thus making cellulose a very strong and stable substance. Nevertheless, there are regions where cellulose microfibrils are packed in a rather unordered manner, often called amorphous regions (Heredia, Jiménez, & Guillén, 1995; Szymanska-Chargot, Cybulska, & Zdunek, 2011).

Hemicelluloses are flexible polysaccharides that characteristically bind to the surface of cellulose microfibrils to tether them in cohesive network. Hemicelluloses come in a wide variety of polymeric structure such as the most abundant xyloglucan (a backbone of cellulose with side chains containing xylose, galactose and fucose) or glucuronoarabinoxylans and glucomannans (Fry, 1988; Taiz & Zeiger, 2002).

Abbreviations: FT-IR, Fourier transform infrared spectroscopy; PCA, principal component analysis; PC, principal component; PLS, partial least squares; RMSECV, root-mean-square error of cross-validation; RMSEC, root-mean-square-error of calibration; CWM, cell wall material; NDF, neutral detergent fibre; ADF, acid detergent fibre; GalA, galacturonic acid; WSP, water soluble pectins; CSP, chelator soluble pectins; DASP, dilute alkali soluble pectins.

* Corresponding author. Tel.: +48 81 744 50 61.
E-mail address: m.szymanska@ipan.lublin.pl (M. Szymanska-Chargot).

http://dx.doi.org/10.1016/j.carbpol.2014.08.039
0144-8617/

Like hemicelluloses, pectins constitute a heterogeneous group of polysaccharides that characteristically contain acidic sugars, such as galacturonic acid, and neutral sugars, such as rhamnose, galactose and arabinose. Pectins are the most soluble of the wall polysaccharides and have the most complicated structure. Pectins form a hydrated gel phase in which the cellulose–hemicellulose network is embedded. They act as a hydrophilic filler, preventing aggregation and collapse of the cellulose network (Carpita & Gibeaut, 1993; Taiz & Zeiger, 2002; Zykwinska, Thibault, & Ralet, 2008).

Although the changes of cell wall polysaccharides have been extensively studied during fruit ripening, little work has been done on the changes during growth and development (Ahmed & Labavitch, 1980; Manrique & Lajolo, 2004; Mangas et al., 1992). During development, when the cellulose microfibrils are synthesized and deposited into a wall, the wall contains high concentrations of other polysaccharides that are able to interact with and perhaps modify growing microfibrils. Previous studies have reported that both pectic and hemicellulosic polysaccharides decreased over time. Fischer and Amado (1994a,b) examined the cell wall changes during the growth and subsequent storage of Golden Delicious apples and found an increase in galacturonic acid, a decrease in neutral sugars, particularly galactose, in the pectic fractions of the cell wall. However, to the best of our knowledge little work has been done on cellulose and hemicellulose changes during development (Lahaye, Quemener, Causse, & Seymur, 2012; O'Donoghue, Huber, Timpa, Erdos, & Becht, 1994; Percy, Melton, & Jameson, 1997).

Usually, the evaluation of cell wall polysaccharide content demands time-consuming, expensive and complex methods. Recently however, FT-IR has found an application in the monitoring of cell wall polysaccharides' extraction, as well as cell wall changes during the processing and quality control of fruits, vegetables or wheat (Barros et al., 2002; Coimbra, Barros, Rutledge, & Delgadillo, 1999; Cozzolino, Cynkar, Shah, Dambergs, & Smith, 2009; Ferreira, Barros, Coimbra, & Delgadillo, 2001; Nawrocka & Cieśla, 2013). For example, the infrared investigation of pectic derivatives allows determining some functional groups which occur in pectic compounds (Barros et al., 2002; Engelsen & Norgaard, 1996). Exploration of region 1800–1600 cm^{-1} offers the possibility of esterification degree estimation (Chatjigakis et al., 1998). Infrared spectroscopy of the main hemicellulosic compounds covers the identification of their specific bands and the assignment of the monosaccharaides constituting these compounds (Gnanasambandam & Proctor, 2000).

Because FT-IR spectra contain very robust information about chemical bonds, it is difficult to obtain compositional information directly from their results. Thus, chemometric techniques such as multivariate models are involved in spectral analysis. These statistical methods help to reduce the data to a scale where the relationship between spectral features and chemical composition can be built. Previous studies using FT-IR spectroscopy combined with principal component analysis (PCA) have proven to be very useful for the fast evaluation of cell wall polysaccharides' composition of pectic and hemicellulosic components derived from plant material when applied in the wavenumber region of 1200–800 cm^{-1} (Coimbra, Barros, Barros, Rutledge, & Delgadillo, 1998; Coimbra et al., 1999; Ferreira et al., 2001; Hori & Sugiyama, 2003; Kačurakova & Wilson, 2001; Winning, Viereck, Salomonsen, Larsen, & Engelsen, 2009). However, the analyses mentioned above were performed most frequently on supernatants containing pectic and hemicellulosic extracts, for example, from olive pulp and sun-dried pear cell walls (Coimbra et al., 1999; Ferreira et al., 2001). Recently, FT-IR spectroscopy connected with multivariate analyses was successfully implemented to enable the rapid quantification of lignocellulosic biomass composition (Hori & Sugiyama, 2003; Chen et al., 2010; Xu, Yu, Tesso, Dowell, & Wang, 2013).

Infrared spectra can effectively represent a 'fingerprint' of the sample being analysed and can be used to simplify methods and reduce analytical times. These advantages, together with the ability to provide detailed chemical information and simultaneously measure several analytes, point to the attractiveness of using such methods. In our previous work, the FT-IR spectroscopy of cell wall bulk residues of sequential extraction connected with PCA analysis showed the wavenumbers which differentiated either the cell wall residue itself or fruit and vegetable species (Szymanska-Chargot & Zdunek, 2013). The aim of this work was to use the chemometric approach to assess quantitatively the cell wall composition in apples from FT-IR spectra of cell wall material. To reach this goal, cell walls from two apple cultivars at different development stages were studied using FT-IR spectroscopy and chemical reference methods. Multivariate methods, i.e., principal component analysis (PCA), *k*-means clustering and partial least square (PLS) were then used to evaluate the FT-IR spectra in order to classify samples, to analyse time-dependent changes in composition, and to predict the quantitative composition in terms of pectin, hemicellulose and cellulose contents.

2. Materials and methods

2.1. Preparation of cell wall material

Two cultivars of apples (*Malus domestica*, cv. 'Ligol' and 'Szampion') were studied. Apples were collected from five trees of each cultivar in the same orchard located in the Grojec region of Poland in 2012. Trees had homogenous characteristic and were placed in the same orchard block. Sampling place in the tree canopy was random, however, approximately from the same height. Apples were collected at six development stages, at the period close to the optimum harvest window, and at a delayed harvest (Table 1). At every stage, fifteen fruits of similar size and maturity were collected. Additionally, in order to evaluate the developmental stage of apples the iodine test for starch presence of five randomly chosen apples from every sampling date was performed. The apples were cut in half across the equator and were dipped for 1 min in an iodine solution (40 g KI + 10 g I_2 in 1 l distilled water) and dried (Table 1). Photos were taken 15 min after the test.

Samples were cut from the cortex tissue of the apples. Cell wall material (CWM) was isolated using the modified hot alcohol insoluble solids method as proposed by Renard (2005). In brief, the fresh slices of material were ground by several bursts of a kitchen processor (Zauberstab, ESGE, Hockenheim, Switzerland), then dropped in hot alcohol (ethanol 70%, temperature approx. 82–85 °C) and left for 20 min of boiling. Then the material was filtered through a nylon net filter (pore size 11 μm, Millipore) and washed successively in 70% and 96% ethanol until the test for sugar presence using the phenol–sulphuric method of Dubois, Gilles, Hamilton, Rebers, and Smith (1956) was negative. The material was then placed in acetone. The sample was vacuum dried and ground using a ball mill (Retsch MM400) at 20 Hz for 20 min. All chemicals were purchased in Sigma Aldrich with purity of analytical grade.

2.2. Cell wall polysaccharides' content

2.2.1. Hemicellulose and cellulose yield

The modified Van Soest's method was used for hemicellulose and cellulose content determination using a crude fibre extractor FIWE 3 (Velp Scientifica, Italy) (Van Soest, 1963). In this method, the cell wall samples were separated progressively into: NDF (neutral detergent fibre) and ADF (acid detergent fibre).

Standard neutral detergent solution used to neutral detergent fibre extraction contained sodium tetraborate decahydrate,

Table 1
Apple development stages studied in the experiment (DAA—days after anthesis). Photos present iodine test for starch content at the development stages.

Stage	T1	T2	T3	T4
Date	3rd July	2 weeks after T1	2 weeks after T2	2 weeks after T3
DAA	59	73	87	101
Ligol				
Szampion				
Stage	T5	T6	T7	T8
Date	1 weeks after T4	1 weeks after T5	1 weeks after T6	1 weeks after T7
Daa	108	115	122	129
Ligol				
Szampion				

ethylenediaminetetraacetic acid (EDTA), sodium dodecyl sulfate (SDS), 2-ethoxyethanol, disodium phosphate anhydrous and sodium sulphite diluted in distilled water; whereas acid detergent solution contained hexadecyltrimethylazanium bromide and sulphuric acid 96%. All chemicals were purchased from Sigma Aldrich with purity of analytical grade.

In brief, approx. 100 mg of cell wall material (m_{CWM}) was placed in an extraction vessel and 100 ml of neutral detergent was added. Then the sample was boiled for 60 min, filtrated and washed in triplicate with boiling water. The residue was dried overnight at 105 °C and finally weighed and left to further step of extraction. The obtained weight was neutral detergent fibre yield (m_{NDF}) and consisted of cellulose and hemicellulose. Refluxing the sample material with neutral detergent solution removed the water-soluble matter and materials other than the fibrous component.

The next step of extraction was conducted with acid detergent solution. 100 ml of acid detergent solution was added to the NDF residue, heated and left at boiling for 60 min. After that it was filtrated and washed in triplicate with boiling water. Refluxing the material with acid detergent solution removed the hemicelluloses. The remaining material was filtrated and dried overnight in 105 °C and finally weighed. The obtained weight was acid detergent fibre yield (m_{ADF}) and consisted of cellulose.

The hemicellulose yield was estimated:

$$H\% = \frac{m_{NDF} - m_{ADF}}{m_{CWM}} \quad (1)$$

and cellulose:

$$C\% = \frac{m_{ADF}}{m_{CWM}} \quad (2)$$

Additionally, taking into account that the cell wall material used for analysis consisted of in particular three components, i.e. pectins, hemicelluloses and cellulose, the total pectic substance could be estimated as:

$$P\% = \frac{m_{CWM} - m_{NDF}}{m_{CWM}} \quad (3)$$

Extractions were triplicated. All the results were expressed as a percentage of cell wall material dry weight.

2.2.2. Galacturonic acid yield

Galacturonic acid (GalA) content was determined after pectin extraction using the method proposed by Redgwell, Curti, and Gehin-Delval (2008) with some modifications. The CWM (100 mg) was stirred firstly in 9 ml of deionized water then filtered, at that point water-soluble pectins (WSP) were obtained. The residue was stirred in 0.1 M *trans*-1,2-diaminocyclohexane-*N*,*N*,*N*′,*N*′-tetraacetic acid, (CDTA, pH 6.5, 5 ml) at 25 °C for 6 h. Then it was filtered and the residue was dissolved in 0.05 M CDTA (pH 6.5, 5 ml), stirred at 25 °C for another 2 h and again filtered. The supernatant of this step was chelator soluble pectins (CSP). Then, the remaining residue was stirred in 0.05 M sodium carbonate (Na_2CO_3) (5 ml) with the addition of 20 mM sodium borohydrite ($NaBH_4$) for approximately 20 h at 1 °C, filtered, and again 5 ml of extracting solution was added to the filtrate and stirred for 2 h at

Table 2
The compositional changes of main components of plant cell wall and their features during apples development. The same superscript letter denotes no significant differences. * means the effect is significant at $p < 0.05$. %P—total pectin yield; %H—hemicellulose yield; %C—cellulose yield; WSP—GalA content in water soluble pectins; CSP—GalA content in chelator soluble pectins; DASP—GalA content in dilute alkali soluble pectins; total GalA–sum of GalA content in all three fractions.

Sample	%P	%H	%C	WSP	CSP	DASP	Total GalA	
		% of cwm d.w.			mg/g of cwm d.w.			
Szampion	T1	63.91 (± 1.37)^{a,c}	23.51 (±1.08)^{a}	12.58 (±0.50)^{a}	8.67 (±0.21)^{a}	5.63 (±0.26)^{a}	53.29 (±0.50)^{a}	68.07 (±0.45)^{a}
	T2	52.30 (± 1.41)^{b,d}	33.23 (±1.68)^{b,c}	14.47 (±0.53)^{a,b}	4.21 (±0.24)^{b}	3.27 (±0.03)^{b}	59.26 (±0.33)^{b}	67.01 (±0.42)^{a}
	T3	60.07 (±1.43)^{a}	28.05 (±0.36)^{a,b}	11.88 (±1.72)^{c}	4.02 (±0.48)^{b}	4.61 (±0.42)^{a}	54.36 (±0.12)^{a}	63.89 (±0.69)^{b}
	T4	57.24 (±0.33)^{b,c,d}	28.95 (±0.40)^{b,c}	13.82 (±0.08)^{a}	6.26 (±0.08)^{c}	4.93 (±0.26)^{a}	62.42 (±0.46)^{c}	73.95 (±0.50)^{c}
	T5	61.84 (±1.35)^{a,c}	23.35 (±1.41)^{a}	14.80 (±0.08)^{a,d}	6.53 (±0.27)^{c}	3.36 (±0.03)^{b}	67.81 (±0.68)^{d}	78.00 (±0.78)^{d}
	T6	50.49 (±1.30)^{d}	30.49 (±0.17)^{c}	19.01 (±1.42)^{b,d}	6.85 (±0.11)^{c}	4.38 (±0.40)^{a}	83.07 (±1.06)^{e}	94.81 (±1.39)^{e}
	T7	52.98 (±0.50)^{d}	27.48 (±0.42)^{b,c}	19.54 (±0.64)^{d}	15.81 (±0.15)^{d}	8.30 (±0.16)^{d}	73.95 (±1.26)^{f}	98.37 (±1.39)^{f}
	T8	52.47 (±0.99)^{d}	27.39 (±0.57)^{b,c}	20.13 (±0.57)^{d}	21.36 (±0.07)^{e}	12.91 (±0.21)^{e}	98.03 (±0.39)^{g}	132.57 (±0.49)^{g}
	F value	18.71*	13.76*	22.07*	1992.325*	473.21*	1457.992*	2241.527*
Ligol	T1	52.46 (±1.47)^{a,c}	30.82 (±1.47)^{a}	16.72 (±0.10)^{a}	6.88 (±0.51)^{a}	2.48 (±0.33)^{a}	56.76 (±1.08)^{a}	66.96 (±0.95)^{a}
	T2	47.04 (±0.50)^{b}	39.14 (±0.50)^{b}	13.82 (±0.08)^{b}	4.55 (±0.11)^{b}	2.38 (±0.31)^{a}	69.61 (±1.20)^{b}	76.97 (±1.49)^{b}
	T3	49.16 (±1.59)^{a,b}	36.32 (±1.86)^{b,c}	14.52 (±0.46)^{b}	4.30 (±0.26)^{b}	3.73 (±0.51)^{a}	70.31 (±0.93)^{b}	79.11 (±1.19)^{b}
	T4	50.99 (±1.31)^{a}	34.21 (±1.37)^{a,c}	14.80 (±0.08)^{c}	7.19 (±0.30)^{a}	4.95 (±0.25)^{b}	72.83 (±0.21)^{b}	85.52 (±0.44)^{c}
	T5	47.81 (±1.06)^{b}	34.97 (±0.57)^{c}	17.22 (±0.50)^{a}	6.22 (±0.18)^{a}	9.54 (±0.61)^{c}	84.13 (±1.19)^{c}	100.69 (±1.14)^{d}
	T6	51.31 (±1.41)^{a}	26.98 (±1.29)^{a,d}	21.71 (±0.12)^{c}	11.38 (±0.47)^{c}	14.18 (±0.06)^{d}	99.09 (±1.55)^{d}	125.17 (±1.97)^{e}
	T7	55.48 (±1.30)^{c}	23.93 (±2.11)^{d}	20.59 (±1.03)^{c}	25.09 (±0.04)^{d}	22.57 (±0.71)^{e}	106.54 (±1.62)^{e}	154.95 (±1.73)^{f}
	T8	51.33 (±1.25)^{a}	23.67 (±0.79)^{d}	25.00 (±0.90)^{d}	26.77 (±0.16)^{e}	27.31 (±0.55)^{f}	110.49 (±2.88)^{e}	165.28 (±3.45)^{g}
	F-value	13.402*	55.539*	161.065*	2827.792*	1300.009*	507.092*	1355.026*

20 °C. The supernatant of this step was diluted alkali soluble pectins (DASP).

The chemical analysis of GalA content in the WSP, CSP and DASP fractions was performed using an Automated Wet Chemistry Analyser also known as a Continuous Flow Analyser (San ++, Skalar Analytical, The Netherlands). This is an automated procedure for colorimetric determination of GalA based on the total decomposition of the pectin sample in acidic medium (hydrolysis with sulphuric acid). The obtained products are transformed to furfural derivatives, which when reacting with 3-phenyl phenol form a coloured dye, which is measured at 530 nm (Filisetti-Cozzi & Carpita, 1991). The pectin content is expressed as galacturonic acid content in the dry mass of the cell wall material (mg/g). The sum of the obtained results gave the total GalA content for each sample. All the analyses were conducted in triplicate.

2.3. FT-IR spectroscopy

FT-IR spectra were collected using a Nicolet 6700 FT-IR spectrometer (Thermo Scientific, Waltham, MA, USA) with the Smart *iTR* ATR sampling accessory. Each sample of CWM was applied on the ATR as powder. The spectra were collected over the range 4000–650 cm^{-1}. For each material, ten samples under the same conditions were examined. For each sample, 200 scans were averaged with a spectral resolution of 4 cm^{-1}. Then, for a given material, a final average spectrum was calculated. Baseline corrections, if needed, were performed using Omnic Software (Thermo Scientific). All spectra were normalized at 1015 cm^{-1} the bands corresponding C—O, C—C stretching vibration in pectins. A graphical presentation of spectra was performed using Origin Software (Origin Lab v8.5 Pro, Northampton, USA). Further analyses, for example, calculation of the first derivatives of the spectra, were performed using the Unscrambler 10.1 (Camo Software AS., Norway) program.

2.4. Statistical analysis: Chemometric approach

Although all the samples were scanned in the mid-infrared region of 4000–400 cm^{-1}, only the region 1500–800 cm^{-1} that contained the most valuable spectral information was taken for analysis using multivariate techniques. Discrete wavelengths of FT-IR were treated as variables. All multivariate statistical analyses (principal component analysis, *k*-means and partial least squares regression) were performed using the Unscrambler 10.1 (Camo Software AS., Norway) program.

Prior to further analysis, the raw baseline-corrected FT-IR spectra were pre-processed using the first derivative Savitzky–Golay (1st derivative, 2nd polynomial order).

Principal component analysis (PCA) is one of the most commonly used chemometric methods for data reduction and exploratory analysis of high-dimensional data sets. The main goal of PCA is to obtain a small set of principal components (PC) that explain the greatest amount of variability in these data sets. PCA creates a new sub-space defined by PCs, which is easier to interpret than the original data. It usually allows the recognition and highlighting of characteristics and their correlation to the physicochemical properties of the sample. This method is especially useful in the interpretation of FT-IR spectra which show band diversity and complication depending on the source of the sample. Here the maximum number of components taken for analysis was seven and the algorithm used was NIPALS. A weighting process of data was performed using the standard deviation as the weight.

Additionally, *k*-means clustering with distance calculated as squared Euclidean was performed to obtain partitioning of the data set into clusters which could give additional information about sample grouping. Non-hierarchical clustering is an unsupervised method which works iteratively to group samples based on their similarity based on some measured variables (Hedegaard et al., 2011; MacQueen, 1967). The output is designed to give a class identification for each object (sample). *K*-means methodology is a commonly used clustering technique. The analysis involves starting with a collection of samples that one attempts to group into a *k*-number of clusters based on certain specific distance measurements. The main steps involved in the *k*-means clustering algorithm are given below. This algorithm is initiated by creating *k* different random spectra as starting centroids. The given sample set is first randomly distributed between these *k* different clusters. The initial cluster centroid is then calculated and in *k*-means this centre is identified using averages. As a next step, the distance measurement between each spectrum, within a given cluster, to its respective cluster centroid is calculated. Each spectrum is assigned to a cluster whose centroid is nearest. When all spectra have been assigned to the *k* centroids, a new set of centroids is calculated based on the mean of the spectra associated with each centroid. This process is then reiterated until the assignment does not change and the incremental improvement is below a given threshold.

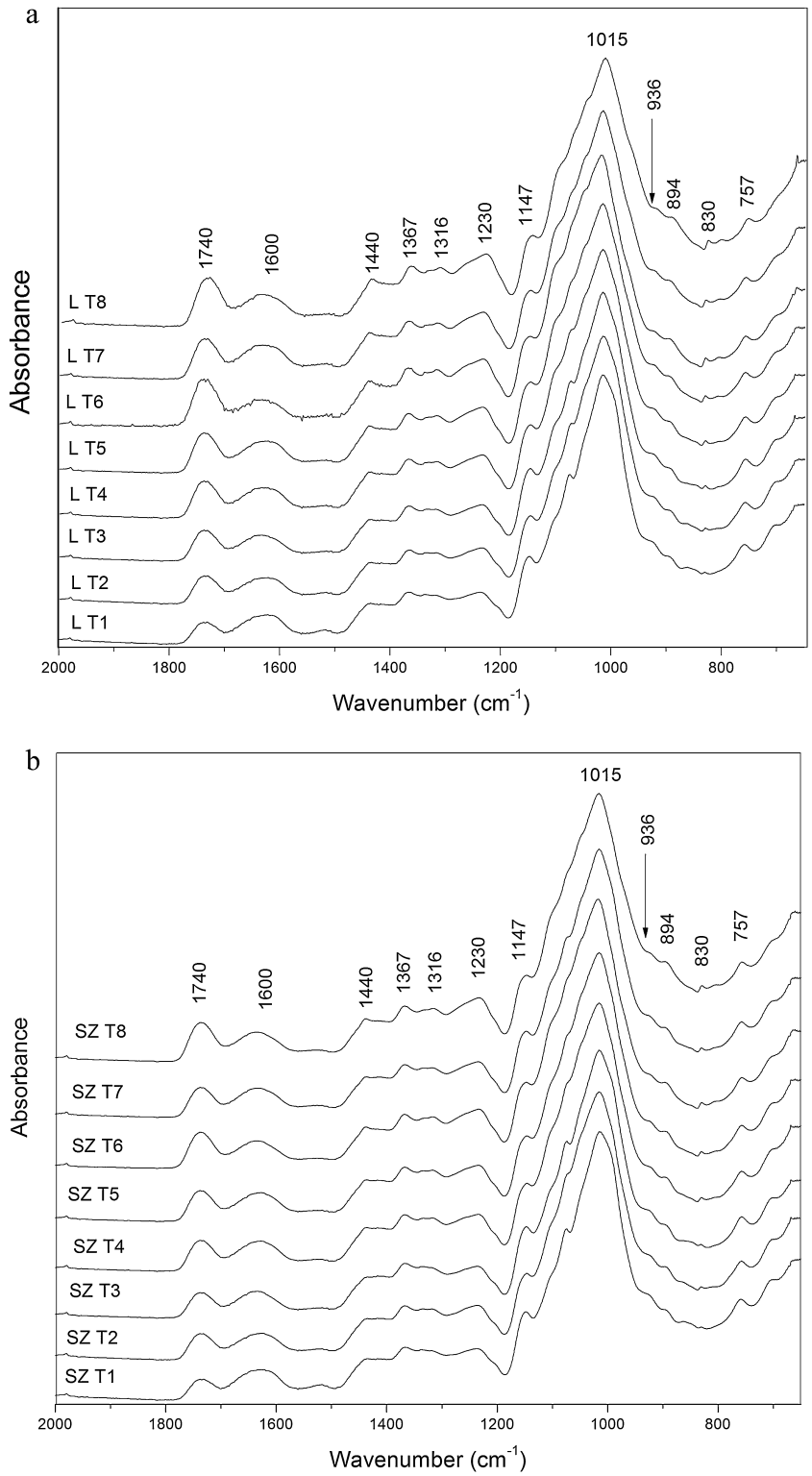

Fig. 1. The FT-IR spectra of cell wall material obtained from the apples of (a) Ligol (L) and (b) Szampion (Sz) cultivars. The bands which are characteristic for cell wall polysaccharides are explained in the text.

The *k*-means algorithm is repeated a number of times to obtain an optimal clustering solution, every time starting with a random set of initial clusters. When an initial starting point is used, only one iteration is run, the default number of iterations to use is 50, and can be adjusted by the user to find the optimal classification. The output of non-hierarchical clustering is a class identifier, based on the proximity of samples to the identified clusters.

Partial least squares regression (PLS) models were developed by utilizing the raw FT-IR spectra as the *X* matrix (predictor) and the reference measurements of contents of pectins, hemicelluloses and cellulose as the *Y* matrix (predicted values). The data of the *X* matrix were mean-centred and variance-scaled, and the *Y* data were only mean-centred. The maximum number of components used for the PLS analysis was seven and the algorithm used

Table 3
Assignment of bands in the infrared spectra of cell wall material from apple parenchyma (Fellah et al., 2009; Kačurakova et al., 2000; Kačurakova & Wilson, 2001; Kondo & Sawatari, 1996; Sene et al., 2004; Synytsya et al., 2003; Wellner, Kačurakova, Malovikova, Wilson, & Belton, 1998; Zhbankov et al., 2002).

Wavenumber (cm^{-1})	Band assignments
1740	C═O stretching vibration of alkyl ester (pectin)
1640	H—O—H bending vibration absorbed water
1600	COO^- antisymmetric stretching polygalacturonic acid, carboxylate (pectin ester group)
1440	asymmetric stretching modes vibration of methyl esters (pectin)
1367	C—H vibrations and CH_2 bending (cellulose, hemicelluloses)
1331	Bending of O—H groups in pyranose ring of pectins
1316	CH_2 symmetric bending or CH_2 rocking vibration (cellulose)
1230	Bending of O—H groups in pyranose ring of pectins
1147	Ring vibrations (C—OH) overlapped with stretching vibrations of side groups and glycosidic bond vibrations (C—O—C) (hemicelluloses)
1000–1200	Skeletal vibrations of the ring or the glycoside bond
1097	C—O stretching, C—C stretching ring pectin
1047	C—O stretching, C—C stretching cellulose (C6—H_2—O6); aromatic C—H in plane deformation
1043	Vibration of arabinose sidechain in pectins
1015	C—O stretching, C—C stretching pectin (C2—C3, C2—O2, C1—O1) backbone vibrations (pectin)
941	Ring vibration (hemicelluloses)
894	Arises in cellulose from the C_1 group frequency or ring frequency, is indicative of β-glycosidic linkages between the sugar unit; antisymmetric out-of-phase ring stretching
830	Out of plan hydroxyl vibrations, vibration of α-linkage (pectins)

was NIPALS. The cross-validation technique was used for model performance testing. The PLS models were evaluated through the root-mean-square error of cross-validation (RMSECV), root-mean-square-error of calibration (RMSEC), and plots of actual versus predicted values. The RMSEC and RMSECV confirm the reliability of the models and should be as small as possible. The value of R^2 was used to explain variance in the model and was the measure of fitting quality. Whereas, Q^2 was used to explain predicted variance and was measure of future prediction quality. These values usually oscillate between 0 and 1, but a value of 0.9 is considered as very good (Eriksson et al., 2006).

The Statistica 10.0 (StatSoft, Inc., Tulusa, OK, USA) program was used for calculation of average values and standard deviations for chemical compositional changes during the development of the apples. Additionally, the effect of harvest data for each cultivar was investigated by analysis of variance (one-way ANOVA) followed by the post hoc Tukey's honestly significant difference (HSD) test for each cultivar independently.

3. Results and discussion

3.1. Content of polysaccharides during development

The content of polysaccharides (pectins, hemicellulose and cellulose) in the cell walls of two apple cultivars was measured as the reference data for further models. Pectin in apples, as the total value and GalA contents, as well as cellulose and hemicellulose overall content are presented in Table 2. From our results it would appear that the total pectin yield (noted in Table 2 as %P) was stable during apple development with $F = 18.48$, $p = 0.000001$ for the 'Szampion' cultivar and $F = 13.40$, $p = 0.000013$ for the 'Ligol' cultivar. The mean content of pectins in the apple cell walls was about 57.76 (±6.09) % of cwm d.w. and 50.63 (±2.79) % of cwm d.w. for the 'Szampion' and 'Ligol' cultivars, respectively. The total pectin value was expressed as the sum of pectin yield in the cell walls containing various pectic polysaccharides. Whereas galacturonic acid was measured in each pectin fraction separately, and a clear increase of GalA in each fraction during fruit development was observed. The largest GalA pectin fraction was DASP which contained from 53.29 (±0.50) mg/g of cwm d.w. to 98.03 (±0.39) mg/g of cwm d.w. and from 56.76 (±1.08) mg/g to 110.49 (±2.88) mg/g, whereas the WSP fraction contained only from 8.67 (±0.21) mg/g up to 21.36 (±0.07) mg/g and from 6.88 (±0.51) mg/g up to 26.77 (±0.16) mg/g of cell wall material dry weight for the 'Szampion' and 'Ligol' cultivars, respectively. This result is evidence that while the fruit is developing galacturonic acid is constantly synthetized.

The content of hemicellulose yield (%H) initially increased, however a decrease could be observed from the 6th development stage. The obtained result is consistent with the previous results obtained by Percy et al. (1997), where on the basis of xylose, fucose and glucose changes, it was assumed that in the early phase of growth, during the rapid cell expansion the amount of xyloglucan increased. Hemicelluloses yield was rather low in the first developmental stage and initially increased (2nd stage). In general, the hemicellulose contribution in the apple cell walls showed a tendency to decrease ($F = 13.76$, $p = 0.000011$) from 33.23 (±1.68) % to 27.39 (±0.57) % for 'Szampion' and ($F = 55.54$, $p = 0$) from 39.14 (±0.50) % to 23.67 (±0.79)% for 'Ligol'. The cellulose content (%C) for both cultivars steadily increased ($F = 22.07$, $p = 0$ for Szampion, and $F = 161.06$, $p = 0$ for Ligol) during development from around 12% to reach 25% of cell wall material dry weight for both cultivars. Moreover, cellulose percentage content exceeded the content of the hemicellulose fraction in the case of the 'Ligol' cultivar.

A simultaneous increase in both galacturonic acid and cellulose content could imply that during fruit growth and cell enlargement cellulose and pectins were synthesized constantly. Percy et al. (1997) stated that a great amount of pectin in the early phase of apple development could mean less structured cell wall growth, which is accompanied with the parallel synthesis of hemicelluloses cross-linking of cellulose microfibrils (Percy et al., 1997). This may lead to the conclusion that the cellulose/hemicellulose load-bearing network became less interlinked, and consequently, together with cell enlargement, resulted in the macroscopic softening of the fruits. Moreover, pectins play a role of plasticizer, which, as was shown previously, softens the composites of cellulose, hemicellulose, and pectins (Cybulska et al., 2010). It was presented that the pure cellulose network produced by bacteria had the highest stiffness whereas the addition of only pectins, or both pectins and xyloglucan, caused significant softening of the composites. Simultaneously with cell wall softening, cell-to-cell adhesion likely increased owing to the increase of GalA in the calcium chelator-soluble pectin fraction (Ng et al., 2013). On the other hand expansin protein is believed to disrupt hydrogen bonding between cellulose microfibrils and matrix polysaccharides. Numerous enzymes and genes are involved in biosynthesis of plant cell wall polysaccharides. Cellulose for instance is formed directly in plasma membrane from spontaneous crystallization of glucose subunit induced by CESA (cellulose synthase) genes (Cosgrove, 2005; Lerouxel, Cavalier, Liepman, & Keegstra, 2006; Vicente, Saladie, Rose, & Labavitch, 2007); whereas matrix polysaccharides are synthesized in Golgi apparatus and then transport to plasma membrane where are integrated with cellulose. In contrast to cellulose, the synthesis of matrix polysaccharides is far more complicated because they possess diverse set of glycosidc linkages and sugar sidechains (Cosgrove, 2005). During fruit developing and physiological ripening different modifications of cell wall polysaccharides could occur (Goulao & Olivieira, 2008). Pectins and hemicelluloses undergo mainly dissolution and depolymerization. Degradation processes could be either enzymatic (enzymes

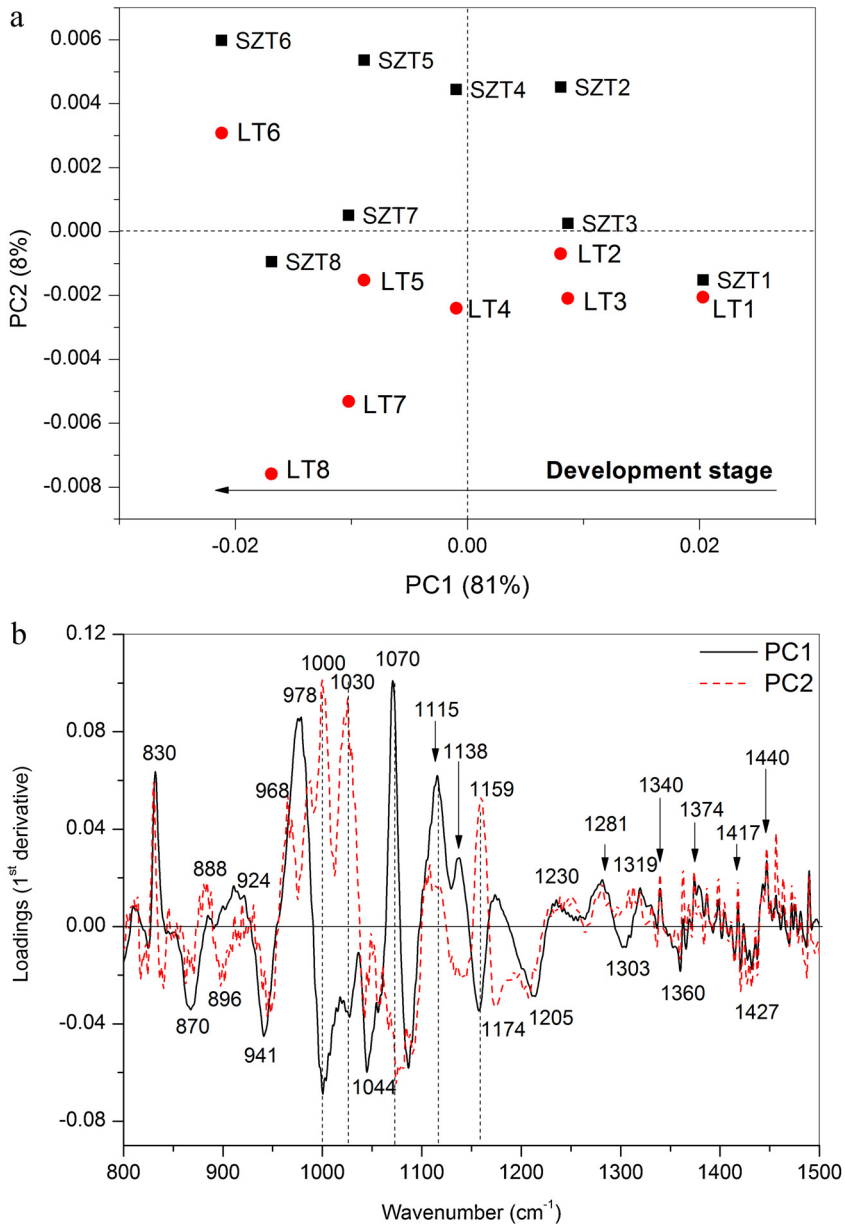

Fig. 2. PCA of the first derivative of FT-IR spectra of cell wall material in the range of (1500–800 cm^{-1}). Scatter of scores (a), loading profile of components PC1 and PC2 (b).

are produced by plant cell and causes polysaccharides hydrolysis) or under action of ascorbic acid, which causes breakdown of cellulose/hemicellulose and cellulose/pectins bonds (Goulao & Olivieira, 2008; Vicente et al., 2007). A little information is available about cellulose content associated with development and ripening, but this polymer is believed to be highly stable (Braam, 1999). However, the correlation between fruit texture of different apple cultivars and their cellulose crystalline state seems to be indispensable (Cybulska et al., 2013).

3.2. Characteristic bands in the FT-IR spectra of apple cell wall polysaccharides

The FT-IR spectra of CWM obtained from the apples regarding their development stage are presented in Fig. 1. Detailed peak positions and assignments of cell wall samples were limited to the 1800–700 cm^{-1} region and are listed in Table 3 (Fellah, Anjukandi, Waterland, & Williams, 2009; Kačurakova, Capek, Sasinkova, Wellner, & Ebringerova, 2000; Kačurakova & Wilson, 2001; Kondo & Sawatari, 1996; Sene, McCann, Wilson, & Grinter, 2004; Synytsya, Čopikova, Matějka, & Machovič, 2003; Wellner, Kačurakova, Malovikova, Wilson, & Belton, 1998; Zhbankov et al., 2002). This region is composed of characteristic band vibrations for the main polysaccharides from the primary plant cell walls. The bands at 1740 and 1600 cm^{-1} are characteristic for esterified and non-esterified carboxyl groups in pectins, respectively. However, this region is also affected by the H—O—H bending vibration of absorbed water. Other characteristic bands for pectins are: 1440, 1331, 1230, 1097, 1015 and 830 cm^{-1}. The bands centred at 1316, 1047 and 899 cm^{-1} are featured as the vibration of characteristic groups in cellulose. The bands which could be assigned for hemicellulosic compounds are 1147, 936 and 757 cm^{-1}. Nevertheless, there are some bands in the spectra of cell wall material which could be assigned to the contribution of a few polysaccharides, such as 1367 cm^{-1} which is characteristic both for cellulose and hemicelluloses, probably because of their similar molecular composition. Moreover, some bands of one substance could be overlapping and influenced by bands in the neighbouring positions, for example,

the pectin band at 1600 cm^{-1} is strongly affected by absorbed water, or the region of 900–1200 cm^{-1} which is characterized by the occurrence of different polysaccharide bands (Fig. 1). The most prominent bands observed which could give information about the composition of cell wall material may be 830, 899 and 934 cm^{-1}, which are wavelengths present in the FT-IR spectra of pectins, cellulose and hemicellulose, respectively. The band centred at 830 cm^{-1} denotes the ring vibration of the α-linkage between (1,4)galacturonic acid units which is the backbone upon which most pectins are built. Therefore, the intensity of this band could reflect not only galacturonic acid content but also the trend in pectin content changes. The band centred at 899 cm^{-1} arises in the cellulose from the C_1 group vibrations or ring vibrations and is indicative of β-glycosidic linkages between the sugar units, hence would be proportional to the cellulose content in the sample. Meanwhile, the band around 934 cm^{-1} could be assigned as ring vibration in the hemicellulose backbone. It is present both for xyloglucan and glucomannan, and could give information about hemicellulose content.

3.3. Principal component analysis (PCA)

The plot of the scores of PCs allows recognition of different groups of samples. Fig. 2a presents the scatter plot of the scores of the first two principal components PC1 and PC2, which together explain 89% of variability. The scores are scattered along both axis: PC1 and PC2. The grouping effect of scores could be observed on both axes. Along the PC1 axis the samples are scattered due to their development stage, and comparing with results in Table 2, it could be stated that are also scattered due to increasing GalA content and cellulose content. Along PC2 axis samples seemed to be grouped according to cultivar.

The loads of the PC1 and PC2 plots vs. wavenumber (Fig. 2b) provide information about the relationship between scores and variables. The loadings of PC1 and PC2 reveal a similar pattern. Positive loadings for PC1 cover wavenumbers characteristic mostly for pectins (830, 888, 1230 and 1440 cm^{-1}) and some for cellulose (1319 and 1340 cm^{-1}) and hemicelluloses (1374 and 1417 cm^{-1}). The negative high values of PC1 were obtained for wavenumbers around 870 and 941 cm^{-1} characteristic for hemicelluloses (glucomannan and xyloglucan, respectively) and for 1000, 1030 1205, 1360 and 1427 cm^{-1}—bands characteristic for cellulose. Therefore, it could be concluded from analysis of PC1 loadings that the negative scores along the PC1 are mainly influenced by cellulose and hemicellulose content. The second factor influencing positively PC1 may be the GalA content which also significantly changed during development period (Table 2) and this is reflected as the major loadings denoting wavenumber characteristics for pectin possessing strong positive influence on the PC1 scores. Fig. 3a and b presents the relationship between PC1 components scores vs. GalA and cellulose content, respectively. In both cases, a clear negative relationship between PC1 scores and total GalA and cellulose content was observable. This fact combined with information acquired from the loadings of PC1 confirmed that indeed the scores along the PC1 axis are scattered due to content of total GalA and cellulose.

The PC2 positive loadings pattern, shown in Fig. 2b, is quite similar to those for PC1, but there are additional bands characteristic for cellulose (1000 and 1030 cm^{-1}) which positively influenced the PC2 scores. The wavenumbers which negatively influenced scores for PC2 are characteristic mainly for cellulose (1000, 1030, 1044, 1159, 1205 and 1427 cm^{-1}) and for hemicelluloses (870, 941, 1205 and 1303 cm^{-1}).

3.4. K-means clustering

The primary purpose of the *k*-means method is presenting data in a manner that emphasizes the natural grouping and

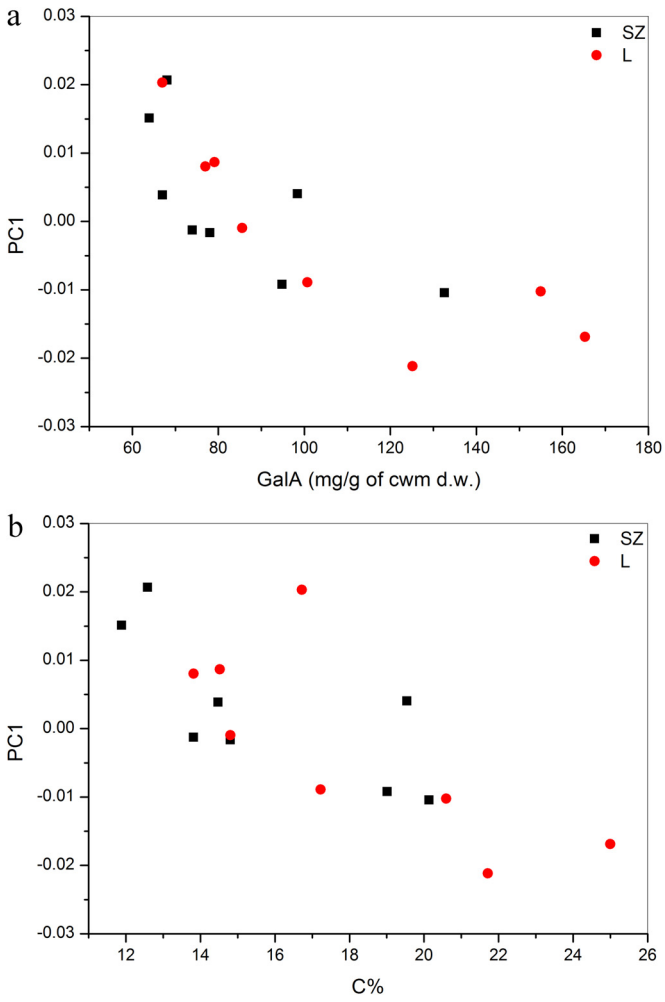

Fig. 3. Relationship between PC1 component scores and (a) galacturonic acid (mg/g) and (b) cellulose (% of cell wall material dry weight) content.

makes it possible to visualize clustering to show the relationships among different groups (Chen et al., 2010; Krasznai, Champagne, & Cunningham, 2012; MacQueen, 1967; Hedegaard et al., 2011). In this work, the *k*-means cluster analysis with the squared Euclidean distance as the similarity measurement gave two clusters dividing 16 samples for two groups: cluster 1 consisted of LT1, LT2, LT3, SZT1, SZT2, SZT3 and SZT7, and the cluster 2 consisting of LT4, LT5, LT6, LT7, LT8, SZT4, SZT5, SZT6 and SZT8. The obtained results are consistent with the PCA model where the scores included in the cluster 1 are grouped on the positive side of the PC1 axis, and included in cluster 2—on the negative side of PC2. The only outlier is the point denoting a sample SZT7, which was classified as cluster 1 but lying on the negative side of the PC1 axis.

3.5. PLS models

The PLS model was built in order to predict of cell wall composition in terms of cellulose, hemicelluloses and galacturonic acid content from FT-IR spectra. An attempt to obtain the PLS model for total pectin content did not provide satisfactory results, therefore the results of this are not presented here. The first derivative of FT-IR spectra in the range of 800–1500 cm^{-1} was taken as the *X* matrix and attributed as predictor or independent variables. The results from the chemical analysis, i.e., galacturonic acid content, hemicelluloses and cellulose content, were taken as the *Y* matrix and attributed as predicted or dependent variables. Due to the

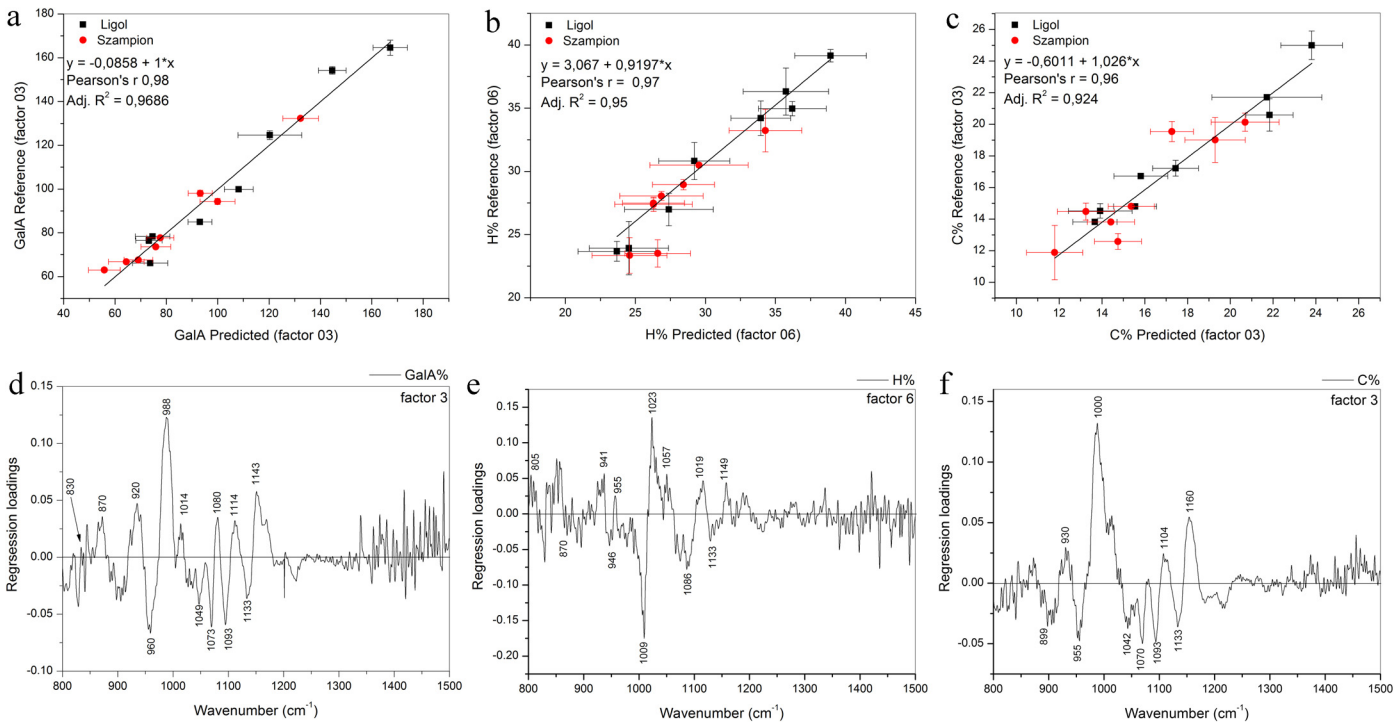

Fig. 4. Predicted vs. reference content of total galacturonic acid in mg/g of cell wall material dry weight (a), hemicellulose in % of cell wall material dry weight (b) and cellulose in % of cell wall material dry weight (c), respectively. The (d)–(f) figures present respective regression loading distributions for the FT-IR wavenumbers.

relative small number of samples, the leaving-one-out cross-validation using seven factors (often called latent variables) was applied.

Fig. 4 presents the predicted vs. the actual galacturonic acid, hemicellulose and cellulose content in the cell walls of the apples. In the case of the PLS model for GalA, the difference between the actual content and predicted values is quite small. The Pearson's R correlation coefficients for the fitting curve were 0.98 for galacturonic acid, 0.97 for hemicellulose and 0.96 for cellulose (Table 4, Fig. 4a–c). In general, the models showed good predictive ability. Each model explained more than 90% of the sample variability ($R^2 > 0.9$) used for model construction, however a particularly high prediction performance was obtained for galacturonic acid ($Q^2 = 0.94$). For cellulose content the Q^2 value was 0.79, and for hemicellulose 0.35. These statistics show that the GalA and cellulose content could be satisfactory predicted using these models, whereas the prediction of hemicellulose from FT-IR spectra is still questionable.

To obtain information on which wavenumbers have the greatest influence on the PLS models, regression loadings for the chosen PLS factors against wavenumber were plotted (Fig. 4d–f). The regression loadings show the relationship between the specified component and the different wavenumbers (Robic, Bertrand, Sassi, Lerat, & Lahaye, 2009). The variables with either positive or negative loading are responsible for the greatest differences between samples, i.e., influence the model the most. The wavenumbers with the high regression loadings for each model are marked in Fig. 4d–f. The most significant wavenumbers for the models are located in the region from 800 to 1200 cm^{-1}; above 1200 cm^{-1} practically only noise could be found. The comparison of the regression loadings for galacturonic acid and cellulose prediction shows slightly similar profiles, which is probably connected to the fact that correlations between their content variations exist. The most important wavenumbers for the prediction of galacturonic acid were 830 cm^{-1} (ring vibration of the α-linkage between (1,4)galacturonic acid units), 920 cm^{-1} (ester groups), 1014 cm^{-1} (stretching of C—O, C—C in galacturonic acid) and 1043 cm^{-1} (vibration of arabinose sidechain) (Coimbra et al., 1998; Filipov, 1972) with positive loadings and bands around wavenumbers 1049 cm^{-1}, 1073 cm^{-1} and 1093 cm^{-1} which are mainly attributed to the ring vibrations with negative loadings. In the case of cellulose regression loadings with positive values, these are located between 1000 cm^{-1}, 1104 (skeletal vibrations) cm^{-1} and 1160 (antisymmetric stretching of C—O—C) cm^{-1}, whereas negative values are similar to those attributed to pectins (1049 cm^{-1}, 1073 cm^{-1} and 1093 cm^{-1}). In the case of hemicellulose content, the positive peaks on the regression loading graph corresponded to the wavenumber characteristics for hemicelluloses (805, 941, 1019 and 1149 cm^{-1}); however, it is difficult to assign wavenumbers corresponding to negative loadings. Part of the wavenumbers which were detected in PLS, and were visible as peaks on the regression loading graphs obtained for individual polysaccharides, were not present on the spectra FT-IR of cell wall material (Fig. 1). This is due to the complexity of cell wall material which causes the overlapping of band characteristics. However, PLS analysis revealed these bands which could be used in the future for quantitative analysis of the cell wall components.

Table 4
Performance statistics of PLS model (details to be found in text) obtained for total galacturonic acid, hemicelluloses and cellulose.

	Total GalA (mg/g of cwm d.w.)	H% of cwm d.w.	C% of cwm d.w.
RMSEC	5.31	1.18	1.04
RMSECV	8.30	4.08	1.74
R^2	0.97	0.94	0.91
Q^2	0.94	0.35	0.79
Pearson's R^2	0.98	0.97	0.96

4. Conclusions

The aim of this work was to compare the results obtained from the chemical analysis of plant cell wall polysaccharide content and their changes during apple development with the results obtained

from FT-IR spectra. It was shown that FT-IR spectroscopy coupled with multivariate methods could be used for both qualitative and quantitative analysis of the cell wall material of the apple parenchyma. The PCA model discriminated samples according to the cultivar, galacturonic acid and cellulose content, whereas *k*-means clustering grouped samples according to the cultivar and development stage. The PLS calibration models for galacturonic acid, hemicelluloses and cellulose content were developed on the basis of FT-IR spectra. The cross-validation errors of the models were very satisfactory: 8.30 mg/g, 4.08% and 1.74% of cell wall material dry weight for galacturonic acid, hemicellulose and cellulose, respectively. Although the variance (R^2) was above 0.9 for each model, the predicted variance of future fitting (Q^2) was satisfactory for the galacturonic acid and cellulose measure using the FT-IR spectra.

Acknowledgments

The research was founded by the Polish National Centre of Science (NCN) (research grant no. 2011/01/D/NZ9/02494).

References

Ahmed, A., & Labavitch, J. M. (1980). Cell wall metabolism in ripening fruit. 1. Cell wall changes in ripening Bartlet pears. *Plant Physiology*, *65*, 1009–1013.
Barros, A. S., Mafra, I., Ferreira, D., Cardoso, S., Reis, A., Lopes da Silva, J. A., et al. (2002). Determination of the degree of methylesterification of pectic polysaccharides by FT-IR using an outer product PLS1 regression. *Carbohydrates Polymers*, *50*, 85–94.
Billy, L., Mehinagic, E., Royer, G., Renard, C. M. G. C., Arvisenet, G., Prost, C., et al. (2008). Relationship between texture and pectin composition of two apple cultivars during storage. *Postharvest Biology and Technology*, *47*, 315–324.
Braam, J. (1999). If walls could talk: Commentary. *Current Opinion in Plant Biology*, *2*, 521–524.
Brownlee, I. A. (2011). The physiological roles of dietary fiber. *Food Hydrocolloids*, *25*, 238–250.
Carpita, N. C., & Gibeaut, D. M. (1993). Structural models of primary cell walls in flowering plants: Consistency of molecular structure with the physical properties of the walls during growth. *The Plant Journal*, *3*(1), 1–30.
Chatjigakis, A. K., Pappas, C., Proxenia, N., Kalantzi, O., Rodis, P., & Polissiou, M. (1998). FT-IR spectroscopic determination of the degree of esterification of cell wall pectins from stored peaches and correlation to textural changes. *Carbohydrate Polymers*, *37*, 395–408.
Chen, H., Ferrari, C., Angiuli, M., Yao, J., Raspi, C., & Bramanti, E. (2010). Qualitative and quantitative analysis of wood samples by Fourier transform infrared spectroscopy and multivariate analysis. *Carbohydrate Polymers*, *82*, 772–778.
Coimbra, M. A., Barros, A., Barros, M., Rutledge, D. N., & Delgadillo, I. (1998). Multivariate analysis of uronic acid and neutral sugars in whole pectic samples by FT-IR spectroscopy. *Carbohydrate Polymers*, *37*, 241–248.
Coimbra, M. A., Barros, A., Rutledge, D. N., & Delgadillo, I. (1999). FTIR spectroscopy as a tool for the analysis of olive pulp cell-wall polysaccharide extracts. *Carbohydrate Research*, *317*, 145–154.
Cosgrove, D. J. (2005). Growth of the plant cell wall. *Nature Reviews*, *6*, 850–861.
Cozzolino, D., Cynkar, W. U., Shah, N., Dambergs, R. G., & Smith, P. A. (2009). A brief introduction to multivariate methods in grape and wine analysis. *International Journal of Wine Research*, *1*, 123–130.
Cybulska, J., Vanstreels, E., Ho, Q. T., Courtin, C. M., Van Craeyveld, V., Nicolaï, B., et al. (2010). Mechanical characteristics of artificial cell walls. *Journal of Food Engineering*, *96*, 287–294.
Cybulska, J., Zdunek, A., Psonka-Antonczyk, K. M., & Stokke, B. T. (2013). The relation of apple texture with cell wall nanostructure studied using an atomic force microscopy. *Carbohydrate Polymers*, *92*, 128–137.
Dubois, M., Gilles, K. A., Hamilton, J. K., Rebers, P. A., & Smith, F. (1956). Colorimetric method for determination of sugars and related substances. *Analytical Chemistry*, *28*, 350–356.
Engelsen, S. B., & Norgaard, L. (1996). Comparative vibrational spectroscopy for determination of quality parameters in amidated pectins as evaluated by chemometrics. *Carbohydrate Polymers*, *30*, 9–24.
Eriksson, L., Johansson, E., Kettaneh-Wold, N., Trygg, J., Wikström, C., & Wold, S. (2006). *Multi- and megavariate data analysis, part 1. Basic principles and applications* (2nd ed.). Sweden: Umetrics AB.
Fellah, A., Anjukandi, P., Waterland, M. R., & Williams, M. A. K. (2009). Determining the degree of methylesterification of pectin by ATR/FT-IR: Methodology optimisation and comparison with theoretical calculations. *Carbohydrate Polymers*, *78*, 847–853.
Ferreira, D., Barros, A., Coimbra, M. A., & Delgadillo, I. (2001). Use of FT-IR spectroscopy to follow the effect of processing in cell wall polysaccharide extracts of a sun-dried pear. *Carbohydrates Polymers*, *45*, 175–182.
Filipov, M. P. (1972). IR spectra of pectin films. *Zhurnal Prikladnoi Spektroskopii*, *17*, 296–299.
Fischer, M., & Amado, R. (1994a). Changes in the pectic substances of apples during development and postharvest ripening. Part 1: Analysis of the alcohol-insoluble residue. *Carbohydrates Polymers*, *25*, 161–166.
Fischer, M., & Amado, R. (1994b). Changes in the pectic substances of apples during development and postharvest ripening. Part 2: Analysis of the pectic fractions. *Carbohydrates Polymers*, *25*, 167–175.
Filisetti-Cozzi, T. M. C. C., & Carpita, N. C. (1991). Measurement of uronic acids without interference from neutral sugars. *Analytical Biochemistry*, *197*, 157–162.
Fry, S. C. (1988). *The growing plant cell wall: chemical and metabolic analysis*. UK: The Blackburn Press, Longman Scientific & Technical.
Gnanasambandam, R., & Proctor, A. (2000). Determination of pectin degree of esterification by diffuse reflectance Fourier transform infrared spectroscopy. *Food Chemistry*, *68*, 327–332.
Goulao, L. F., & Olivieira, C. M. (2008). Cell wall modifications during fruit ripening: When a fruit is not the fruit. *Trends in Food Science& Technology*, *19*, 4–25.
Hedegaard, M., Matthäus, C., Hassing, S., Krafft, C., Diem, M., & Popp, J. (2011). Spectral unmixing and clustering algorithms for assessment of single cells by Raman microscopic imaging. *Theoretical Chemistry Accounts*, *130*, 1249–1260.
Heredia, A., Jiménez, A., & Guillén, R. (1995). Composition of plant cell walls. *Zeitschrift für Lebensmittel Untersuchung und Forschung*, *200*, 24–31.
Hori, R., & Sugiyama, J. A. (2003). Combined FT-IR microscopy and principal component analysis on softwood cell walls. *Carbohydrate Polymers*, *52*, 449–453.
Kačurakova, M., Capek, P., Sasinkova, V., Wellner, N., & Ebringerova, A. (2000). FT-IR study of plant cell wall model compounds: Pectic polysaccharides and hemicelluloses. *Carbohydrate Polymers*, *43*, 195–203.
Kačurakova, M., & Wilson, R. H. (2001). Developments in mid-infrared FT-IR spectroscopy of selected carbohydrates. *Carbohydrate Polymers*, *44*, 291–303.
Kondo, T., & Sawatari, Ch. (1996). A Fourier transform infra-red spectroscopic analysis of the character of hydrogen bonds in amorphous cellulose. *Polymer*, *37*, 393–399.
Krasznai, D. J., Champagne, P., & Cunningham, M. F. (2012). Quantitative characterization of lignocellulosic biomass using surrogate mixtures and multivariate techniques. *Bioresource Technology*, *110*, 652–661.
Lahaye, M., Quemener, B., Causse, M., & Seymur, G. B. (2012). Hemicellulose fine structure is affected differently during ripening of tomato lines with contrast texture. *International Journal of Biological Macromolecules*, *51*, 462–470.
Li, Z., Yang, H., Li, P., Liu, J., Wang, J., & Xu, Y. (2013). Fruit biomechanics based on anatomy: A review. *International Agrophysics*, *27*, 97–106.
Lerouxel, O., Cavalier, D. M., Liepman, A. H., & Keegstra, K. (2006). Biosynthesis of plant cell wall polysaccharides—A complex process. *Current Opinion in Plant Biology*, *9*, 621–630.
MacQueen, J. (1967). Some methods for classification and analysis of multivariate observations. In *Berkeley symposium on mathematical statistics and probability* (pp. 287–297).
Mangas, J. J., Dapena, E., Rodiguez, M. S., Moreno, J., Gutierrez, M. D., & Blanco, D. (1992). Changes in pectic fractions during ripening of cider apples. *HortScience*, *27*, 328–330.
Manrique, G. D., & Lajolo, F. M. (2004). Cell-wall polysaccharide modifications during postharvest ripening of papaya fruit (*Carica papaya*). *Postharvest Biology and Technology*, *33*, 11–26.
Nawrocka, A., & Cieśla, J. (2013). Influence of silver nanoparticles on food components in wheat. *International Agrophysics*, *27*, 49–55.
Ng, J. K., Schröder, R., Sutherland, P. W., Hallett, I. C., Hall, M. I., Prakash, R., et al. (2013). Cell wall structures leading to cultivar differences in softening rates develop early during apple (Malus × domestica) fruit growth. *BMC Plant Biology*, *13*, 183.
O'Donoghue, E. M., Huber, D. J., Timpa, J. D., Erdos, G. W., & Becht, J. K. (1994). Influence of avocado (*Persea americana*) Cx-cellulase on the structural features of avocado cellulose. *Planta*, *194*, 573–584.
Phillips, G. O., & Cui, S. W. (2011). An introduction: Evolution and finalization of the regulatory definition of dietary fiber. *Food Hydrocolloids*, *25*, 139–143.
Percy, A. E., Melton, L. D., & Jameson, P. E. (1997). Xyloglucan and hemicelluloses in the cell wall during apple fruit development and ripening. *Plant Science*, *125*, 31–39.
Redgwell, R. J., Curti, D., & Gehin-Delval, C. (2008). Physicochemical properties of cell wall materials from apple, kiwifruit and tomato. *European Food Research and Technology*, *227*, 607–618.
Renard, C. M. G. C. (2005). Variability in cell wall preparations: Quantification and comparison of common method. *Carbohydrate Polymers*, *60*, 512–522.
Robic, A., Bertrand, D., Sassi, J.-F., Lerat, Y., & Lahaye, M. (2009). Determination of the chemical composition of ulvan, a cell wall polysaccharide from Ulva spp. (Ulvales, Chlorophyta) by FT-IR and chemometrics. *Journal of Applied Phycology*, *21*, 451–456.
Sene, C. F. B., McCann, M. C., Wilson, R. H., & Grinter, R. (2004). Fourier-transform Raman and Fourier-transform infrared spectroscopy. An investigation of five higher plant cell walls and their components. *Plant Physiology*, *106*, 1623–1631.
Synytsya, A., Čopikova, J., Matějka, P., & Machovič, V. (2003). Fourier transform Raman and infrared spectroscopy of pectins. *Carbohydrate Polymers*, *54*, 97–106.
Szymanska-Chargot, M., Cybulska, J., & Zdunek, A. (2011). Sensing the structural differences in cellulose from apple and bacterial cell wall materials by Raman and FT-IR spectroscopy. *Sensors*, *11*, 5543–5560.
Szymanska-Chargot, M., & Zdunek, A. (2013). Use of FT-IR spectra and PCA to the bulk characterization of cell wall residues of fruits and vegetables along a fraction process. *Food Biophysics*, *8*, 29–42.

Taiz, L., & Zeiger, E. (2002). *Plant physiology* (3rd ed.). Sunderland: Sinauer Associates (Chapter 15).
Wellner, N., Kačurakova, M., Malovikova, A., Wilson, R. H., & Belton, P. S. (1998). FT-IR study of pectate and pectinate gels formed by divalent cations. *Carbohydrate Research*, *308*, 123–131.
Willats, W. G. T., Knox, J. P., & Mikkelsen, J. D. (2006). Pectin: New insights into an old polymer are starting to gel. *Trends Food Science and Technology*, *17*(3), 97–104.
Winning, H., Viereck, N., Salomonsen, T., Larsen, J., & Engelsen, S. B. (2009). Exploring abiotic stress on asynchronous protein metabolism in single kernels of wheat studied by NMR spectroscopy and chemometrics. *Carbohydrate Research*, *344*, 1833–1841.
Van Soest, P. J. (1963). Use of detergents in the analysis of fibrous feeds. II. A rapid method for determination of fiber and lignin. *Journal of the Association of Official Analytical Chemists*, *46*, 155–160.
Vicente, A. R., Saladie, M., Rose, J. K. C., & Labavitch, J. M. (2007). The linkage between cell wall metabolism and fruit softening: Looking to the future. *Journal of the Science of Food and Agriculture*, *87*, 1435–1448.
Xu, F., Yu, J., Tesso, T., Dowell, F., & Wang, D. (2013). Qualitative and quantitative analysis of lignocellulosic biomass using infrared techniques: A mini-review. *Applied Energy*, *104*, 801–809.
Zhbankov, R. G., Firsov, S. P., Buslov, D. K., Nikonenko, N. A., Marchewka, M. K., & Ratajczak, H. (2002). Structural physico-chemistry of cellulose macromolecules. Vibrational spectra and structure of cellulose. *Journal of Molecular Structure*, *614*, 117–125.
Zykwinska, A., Thibault, J.-F., & Ralet, M.-C. (2008). Competitive binding of pectin and xyloglucan with primary cell wall cellulose. *Carbohydrate Polymers*, *74*, 957–961.